

1 **Design of Multifunctional Nanostructure for Ultrafast Extraction**
2 **and Purification of Aflatoxins in Foodstuffs**

3
4 **Jie Xie ^{†,1}, Haiyang Jiang ^{†,1}, Jianzhong Shen [†], Tao Peng [†], Jianyi Wang [†], Kai Yao [†],**
5 **Shujuan Sun [†], Bing Shao ^{*,†}, Junwang Tang ^{*,‡}**

6
7 [†] *Beijing Advanced Innovation Center for Food Nutrition and Human Health, College of*
8 *Veterinary Medicine, China Agricultural University, Beijing 100193, P. R. China*

9 [‡] *Department of Chemical Engineering, University College London, Torrington Place, London*
10 *WC1E7JE, UK*

1 **ABSTRACT:** Aflatoxins (AFs) are a class of carcinogens associated with liver cancers which are
2 used to exist in foodstuffs. There are extremely low maximum limits of AFs in foodstuffs (0.025–
3 20 $\mu\text{g kg}^{-1}$). To fast and sensitively detect such low concentration of AFs in foodstuffs is
4 dominated by the efficiency and selectivity of AFs enrichment process, which is extremely
5 challenging although substantial efforts have been made over the past decades. Here we designed
6 and synthesized a multilayer nanoarchitecture composed of a broad-spectrum AFs monoclonal
7 antibody shell, chitosan middle layer and magnetic bead core (denoted AFs-mAb/CTS/Fe₃O₄).
8 The efficiency of AFs-mAb/CTS/Fe₃O₄ in extracting AFs has been found to be more than 60
9 times higher than both conventional immunoaffinity chromatography and solid-phase extraction.
10 Furthermore, the nanocomposite displays excellent selectivity and good reusability apart from
11 outstanding efficiency. Coupling to ultra-performance liquid chromatography–tandem
12 quadrupole mass spectrometry, this new nanoarchitecture enables to probe six AFs as low as
13 0.003 $\mu\text{g kg}^{-1}$ in foodstuffs with free matrix effects, which is nearly 10 times smaller than the
14 regulated maximum tolerated does. It is believed that the new nanoarchitecture would provide an
15 efficient and fast pathway to detect AFs in foodstuffs to protect human being from some critical
16 liver cancers.

17

1 Liver cancers are the third leading cause of cancer death worldwide, and the fifth commonest
2 cancers in men and the eighth commonest in women.^{1,2} Aflatoxins (AFs) are associated with
3 acute liver damage, liver cirrhosis, the induction of tumors, and teratogenic effects.^{3,4} An
4 extremely tragic event associated with AFs-contaminated foods occurred in Kenya in 2004–2005,
5 when more than 1000 people were poisoned, 120 of whom died.⁵ The most important AFs are
6 AFB₁, AFB₂, AFG₁, AFG₂, AFM₁, and AFM₂.⁶ The International Agency for Research on
7 Cancer (IARC) has classified AFB₁, AFB₂, AFG₁, AFG₂, and AFM₁ as Group 1 human
8 carcinogens.⁷ Unfortunately, these AFs are regularly found in improperly stored staple
9 commodities, including corn, peanuts, rice, tree nuts, wheat, etc.^{7–9} To safeguard human health,
10 almost all countries have set extremely low maximum tolerated limits (MTLs) of AFs in food.¹⁰
11 The MTLs of AFB₁ and of total AFs in food are 5 and 10–20 µg kg⁻¹, respectively, in more than
12 75 countries around the world,^{11,12} whereas they are 2 and 4 µg kg⁻¹, respectively, in the
13 European Union (EU).¹³ Stricter MTLs, as low as 0.1 µg kg⁻¹ for AFB₁ and 0.025 µg kg⁻¹ for
14 AFM₁, are set for infant formulae and infant foods in the EU.¹³ Considering the potential threat of
15 AFs to human health, efficient approaches are urgently required for the rapid and sensitive
16 analysis of those in foodstuffs.

17 At present, liquid chromatography coupled to triple quadrupole mass spectrometry (LC–
18 MS/MS) is frequently used for the analysis of AFs in foods.^{14,15} Despite the universality,
19 sensitivity, and selectivity of the LC–MS/MS method, overcoming the variable matrix effects of
20 electrospray ionization remains a big challenge in this process.⁸ To eliminate signal suppression
21 or enhancement, several typical purification techniques have been developed to compensate for
22 matrix effects, such as liquid–liquid extraction (LLE),¹⁶ solid–phase extraction (SPE),¹⁷ and
23 immunoaffinity chromatography (IAC).⁴ However, LLE and SLE usually require a lot of organic

1 solvent, and SPE techniques often involve nonspecific retention. Although IAC can generally
2 produce clean extracts, with small variability between samples, and chromatograms free of
3 matrix interference, the limited flow rate and possible congestion by larger sample particles often
4 cause very long waiting time for the samples analysis.

5 Building on the discovery of functional nanoparticles, immunomagnetic techniques have been
6 used successfully to separate tumor cells,^{18,19} bacteria,²⁰ viruses,²¹ allergens,²² proteins,²³
7 hormones,²⁴ and AFB₁^{25,26} from food matrices, providing attractive alternatives for the rapid
8 concentration and purification of AFB₁. Xie et al.²⁵ used indirect method to immobilize antibody
9 on biotinylated magnetic beads for the pretreatment of AFB₁ in soybean sauce with about 0.5 h of
10 time consuming. Xiong et al.²⁶ also designed a magnetic beads carrying poly (acrylic acid)
11 brushes as “nanobody containers” for immunoaffinity purification of AFB₁ from corn samples.
12 Although high loading and adsorption capacity were available owing to the using of
13 nanoparticles, one hour was needed to capture AFB₁, which was comparative with the
14 conventional IAC method. Chitosan (CTS) has abundant amino (–NH₂) and hydroxyl (–OH)
15 groups for chemical modifications,^{27–29} and has been tried for the separation or purification of
16 heavy metal ions,²⁷ bovine serum albumin (BSA),³⁰ and proteins.³¹ CTS thus has a potential to
17 covalently immobilize magnetic beads and antibodies.

18 Herein we designed a multifunctional nanoarchitecture by integrating magnetic property of
19 Fe₃O₄, functional groups of CTS and selective monoclonal antibody. The nanostructured
20 CTS/Fe₃O₄ were prepared with a simple one-step method and characterized in detail. Further, a
21 broad-spectrum monoclonal antibody directed against six AFs was immobilized on the
22 nanocomposite through the amidocarbonylation reaction, generating the AFs-mAb/CTS/Fe₃O₄
23 adsorbent (Scheme 1). The multifunctional architecture has been validated with standard

1 reference materials for ultrafast (ca. 0.5 min) sample extraction and purification, demonstrating
2 its advances in the fast and efficient detection of ultratrace levels of chemicals in complex food
3 matrices.

4 ■ EXPERIMENTAL SECTION

5 **Materials.** AFB₁, AFB₂, AFG₁, AFG₂, AFM₁, and AFM₂ standards (purity \geq 99%) were
6 purchased from Dr. Ehrenstorfer GmbH (Augsburg, Germany). The monoclonal antibody against
7 AFs (3D10) was prepared in our laboratory (see Supporting Information). FeCl₃·6H₂O, ethylene
8 glycol, sodium acetate, and CTS (\geq 95% deacetylation, with a viscosity average molecular weight
9 of 3.0×10^5 g mol⁻¹) were obtained from Beijing Chemical Reagent Co., Ltd (Beijing, China).
10 *N*-Hydroxysulfosuccinimide (sulfo-NHS), morpholinoethanesulfonic acid (MES),
11 *N*-(3-dimethylaminopropyl)-*N*-ethylcarbodiimide hydrochloride (EDC), and bovin serum
12 albumin (BSA) were purchased from Sigma-Aldrich (St. Louis, MO, USA).

13 **Synthesis of CTS/Fe₃O₄ and Fe₃O₄.** The magnetic particles CTS/Fe₃O₄ and Fe₃O₄ were
14 synthesized and characterized based on the modified solvothermal reduction method.^{27,29} The
15 detailed procedures were given in the Supporting Information.

16 **Characterization.** TEM images of Fe₃O₄ and CTS/Fe₃O₄ were taken with a JEM-2100F
17 field-emission high resolution transmission electron microscope (JEOL Co., Japan). SEM images
18 were scanned by a Merlin Compact field-emission scanning electron microscope equipped with
19 an EDS unit (ZEISS, Germany). XRD patterns were recorded on a Rigaku Dmax/2400
20 diffractometer (Rigaku Co., Japan) with Cu Ka radiation at 40 kV and 200 mA. FTIR spectra
21 were recorded with a Nicolet™ iS™ 50 FTIR spectrometer (Thermo Fisher Scientific, Waltham,
22 MA, USA), with scanning waves ranging from 400 to 4000 cm⁻¹. TGA was performed with a
23 Q600 SDT thermogravimetric analyzer (TA Instruments, USA), under an air flow of 100 mL

1 min⁻¹ at a heating rate of 20 °C min⁻¹.

2 **Preparation of AFs-mAb/CTS/Fe₃O₄.** CTS/Fe₃O₄ nanoparticles (0.1 g) were added to 1.0 mL
3 of MES buffer (0.05 mol L⁻¹, pH 5.0) and mixed thoroughly. Then, 20 μL of EDC (0.5 mg mL⁻¹)
4 and 20 μL of sulfo-NHS (0.5 mg mL⁻¹) were added to the mixture and shaken for 15 min.
5 Anti-AFs mAb (1.0 mg) was mixed with the sulfo-NHS/EDC-treated CTS/Fe₃O₄ solution for 30
6 min. Finally, 20 μL of 20% BSA was added for 10 min to block any excess activated sites. After
7 magnetic separation, the aggregates were resuspended in 2 mL of phosphate buffer (0.05 mol L⁻¹,
8 pH 7.4) containing 0.02% (v/w) sodium azide, 0.5% BSA, and 1% Tween 20. The prepared
9 magnetic immunoadsorbent was stored at 4°C before use. The maximum coupling amount of
10 AFs-mAb on 0.1 g CTS/Fe₃O₄ was monitored with the same method used to prepare
11 AFs-mAb/CTS/Fe₃O₄, except different concentration of AFs-mAb solution (5, 10, 15, 20, 25, 30
12 mg mL⁻¹) was used.

13 **Sample Extraction and Preconcentration.** Corn, rice, wheat, peanut, peanut oil, sunflower
14 oil, olive oil products destined for human consumption were obtained from several supermarkets
15 in Beijing (China). Cereal samples were finely milled using a knife mill Grindomix GM 200
16 (Retsch, Haan, Germany) and homogenized to achieve a representative samples and then
17 dispensed into plastic bags. Vegetable oil samples were directly measured. All samples were
18 stored under cool conditions and out of direct sunlight until the analysis. Samples (25 g) were
19 weighed into 500 mL polypropylene bottles, to which 5 g NaCl was added, and the samples were
20 extracted with 125 mL of methanol–deionized water (60:40, v/v) with vigorous shaking for 30
21 min. The extract was filtered and 20 mL of filtrate was diluted with 120 mL of water. The pH
22 was adjusted to 5.5–6.5. A suspension of immunomagnetic beads (0.3 mL) was then added to 60
23 mL of diluted extract (equivalent to 2.0 g of sample), and shaken gently for 0.5 min to capture the

1 AFs. An external magnet was attached to the outside bottom of the vial and the
2 AFs-mAb/CTS/Fe₃O₄ was gathered to the bottom of the tube. The supernatant was discarded.
3 Water (20 mL) was added to the tube, which was shaken for 10 s. Methanol (1.0 mL) was added
4 and the tube was vortexed for 5 s. The magnet was then attached to the outside bottom of the tube.
5 The supernatant was collected and evaporated to near dryness under a gentle stream of nitrogen at
6 45 °C. The residue was reconstituted with 1.0 mL of the initial mobile phase used in the
7 ultra-performance liquid chromatography coupled to triple quadrupole mass spectrometry
8 (UPLC–MS/MS) analysis. The development and conditions of the UPLC–MS/MS method are
9 given in the Supporting Information.

10 **Applications.** To compare the purification efficacy of the AFs-mAb/CTS/Fe₃O₄
11 immunomagnetic absorbent, SPE, and IAC, three certificated reference materials were purchased
12 from Trilogy Analytical Laboratory (Washington, MO, USA). The procedures for SPE and IAC
13 were provided in the Supporting Information.

14 ■ RESULTS AND DISCUSSION

15 **Synthesis and Characterization of CTS/Fe₃O₄.** The powder X-ray diffraction (XRD) spectra
16 for CTS/Fe₃O₄ are presented in Figure 1a. It has six diffraction peaks, with $2\theta = 30.1^\circ, 35.4^\circ,$
17 $42.9^\circ, 53.5^\circ, 56.9^\circ,$ and 62.6° , corresponding to (220), (311), (400), (422), (511), and (440)
18 planes, respectively, which is consistent with the standard spectra for Fe₃O₄ with an inverse cubic
19 spinel structure.³⁴ The diffraction peaks are highly symmetric and sharp, indicating that the
20 particles were well crystallized. Fe₃O₄ crystal shape remain unchanged during the solvothermal
21 reaction with CTS while, a small peak appears in the range from 17° to 20° , indicating the
22 presence of amorphous CTS.²⁹ The morphology and structure of the CTS/Fe₃O₄ nanospheres
23 were examined with field-emission scanning electron microscopy (SEM) and high-resolution

1 transmission electron microscopy (HR-TEM). SEM images suggested that the CTS/Fe₃O₄
2 nanospheres are spherical with a very narrow size distribution (average particle size of ~200 nm)
3 (Figure 1b), consistent with HR-TEM observation (Figure 1c). The Fe₃O₄ particles of ~200 nm
4 (black region) were successfully coated by the CTS layer with a thickness of ~10 nm (shadow
5 region) (Figure 1c). The fourier transform infrared (FTIR) spectrum (Figure 1d) of CTS was
6 characterized by the following absorption bands: $\nu(\text{C-H})$ of the backbone polymer, around 2871
7 and 2929 cm^{-1} ; $\nu(\text{C-O})$ of the primary alcoholic group, 1377 cm^{-1} ; $\nu(\text{C=O})$ of amide, 1060 cm^{-1} ;
8 and $\delta(\text{N-H})$ of the primary amine, around 3356 cm^{-1} . The spectrum of CTS/Fe₃O₄ is a
9 combination of both CTS and Fe₃O₄ FTIR spectrum, further indicating that CTS was successfully
10 coated onto the surfaces of the Fe₃O₄ nanoparticles. Energy dispersive spectroscopy (EDS)
11 (Figure S1) shows 8.65% (wt.) nitrogen, also implying that the CTS were successfully coated on
12 Fe₃O₄ nanoparticles. The thermal stability of the materials was investigated with a
13 thermogravimetric analysis (TGA) as shown in Figure S2, which indicated that the CTS content
14 of CTS/Fe₃O₄ was about 19.6%.

15 **Preparation and Characterization of AFs-mAb/CTS/Fe₃O₄.** The conditions of the coupling
16 reaction for preparing the immunomagnetic beads were optimized because these conditions may
17 strongly influence CTS–monoclonal antibody (mAb) binding. According to the reported study,³⁵
18 BSA was used as a model protein in the optimization experiment before immobilizing antibody
19 on the solid support material. The final optimized conditions were then applied to the preparation
20 of AFs-mAb/CTS/Fe₃O₄. To optimize the coupling efficiency of the CTS/Fe₃O₄ nanoparticles
21 with the AFs-mAb, different coupling methods were compared, including the glutaraldehyde (GA)
22 method,³⁶ the electrostatic adsorption (ESA) method,³⁰ and the EDC/sulfo-NHS method.³⁷ The
23 coupling efficiency of the GA method was below 30% (Figure 2a), because the reaction solvent

1 used in this method is carbonate buffer (pH 9.0), in which both the CTS/Fe₃O₄ nanoparticles and
2 BSA are negatively charged. The electrostatic adsorption BSA on the CTS/Fe₃O₄ nanoparticles
3 was also investigated. The coupling efficiency of the ESA method was 90%. An explanation for
4 this phenomenon might involve the surface charge on the CTS/Fe₃O₄ nanoparticles and BSA in
5 weak acidic buffer.³⁸ At the isoelectric point, BSA has a negative charge, whereas CTS/Fe₃O₄
6 nanoparticles have a positive charge, and the electrostatic interaction between them is one of the
7 driving forces of the adsorption process.³¹ However, the electrostatic bonding is not very stable,
8 especially when the pH changes or in the presence of other compounds in the solution. The
9 highest coupling efficiency (Figure 2a) was obtained with the EDC/sulfo-NHS method, because it
10 efficiently cross-linked the –COOH groups of BSA or IgG with the –NH₂ groups of CTS without
11 leaving a spacer molecule.³⁸ Therefore, BSA or IgG was conjugated to the CTS/Fe₃O₄
12 nanoparticles with a commonly used biochemical protocol based on EDC/sulfo-NHS, a highly
13 efficient ‘zero-length’ cross-linking agent. The coupling of the CTS/Fe₃O₄ nanoparticles with
14 BSA was also investigated in four coupling solutions of different ionic strength, using the
15 selected EDC/sulfo-NHS method. As shown in Figure 2b, the amount of BSA bound on the
16 CTS/Fe₃O₄ nanoparticles was better (98.3%) in 0.05 mol L⁻¹ MES solution than that in other
17 three binding solutions. Therefore, 0.05 mol L⁻¹ MES was selected as the coupling solution. The
18 effects of pH on the coupling reaction were next studied, as shown in Figure 2c. Various pHs
19 were tested, ranging from 3.0 to 8.0. The pH had a remarkable effect on the coupling of BSA with
20 the CTS/Fe₃O₄ nanoparticles. Under neutral or alkaline conditions, negligible BSA was bound to
21 the CTS/Fe₃O₄ nanoparticles. The maximum adsorption of BSA occurred at approximately pH
22 5.0, which is very close to the isoelectric point of BSA (pI = 4.7).^{39,40} As the pH decreased from
23 5.0 to 3.0, the amount of BSA adsorbed onto the CTS/Fe₃O₄ nanoparticles varied slightly, which

1 can be explained by the low protonation of the $-\text{NH}_2$ groups at high pH.³⁸ Therefore, pH 5.0 was
2 selected as the optimal pH for the coupling reaction. A series of reaction times for the coupling
3 process was also tested. As shown in Figure 2d, the coupling efficiency of BSA to CTS/ Fe_3O_4
4 increased gradually at coupling times of less than 30 min, whereas after 30 min, the CTS/ Fe_3O_4
5 was saturated with BSA. Therefore, 30 min was selected as the coupling time to ensure that the
6 coupling with BSA was at saturation equilibrium. Under the optimized conditions,
7 AFs-mAb/CTS/ Fe_3O_4 nanoparticles were then fabricated. In order to test the maximum coupling
8 amount of AFs-mAb on 0.1 g CTS/ Fe_3O_4 , a set of AFs-mAb solution (5, 10, 15, 20, 25, 30 mg
9 mL^{-1}) was investigated. As illustrated in Figure S3, the maximum amount of AFs-mAb coupled
10 on the magnetic beads was found to be 23.5 mg g^{-1} . When the the coupling amount was 10 mg
11 g^{-1} , the maximum AFs-binding capacities were 337, 351, 306, 113, 462 and 389 ng/mL for AFB₁,
12 AFB₂, AFG₁, AFG₂, AFM₁ and AFM₂ (Figure S4), respectively, which meets the detection
13 requirements. Therefore, 10 mg g^{-1} was selected as the optimum coupling amount and used in the
14 following experiment.

15 **Sample Extraction and Preconcentration.** Negative samples (Corn, rice, wheat, peanut,
16 peanut oil, sunflower oil, olive oil) fortified with each analyte (1.0 $\mu\text{g kg}^{-1}$) were used to
17 investigate the extraction performance of the immunomagnetic beads under different conditions.
18 Results for the extraction of processed corn are given in Figure 3, and slightly different results
19 were obtained in other matrices. Considering all the results, the optimized results of corn sample
20 were selected as the best conditions for every matrix. First, the effect of the amount of
21 immunomagnetic absorbent was investigated in the range 0.1–0.6 mL. As shown in Figure 3a, the
22 extraction recoveries of the targets gradually increased as the amount of AFs-mAb/CTS/ Fe_3O_4
23 immunoabsorbent increased from 0.1 to 0.3 mL, and then remained almost constant at amounts

1 of absorbents > 0.3 mL. Therefore, 0.3 mL of AFs-mAb/CTS/Fe₃O₄ was selected. We then
2 studied the effects of different proportions of methanol in the adsorption solution (0%, 5%, 10%,
3 15%, 20%, 25%, or 30%) during the adsorption step. As shown in Figure 3b, the best recoveries
4 were obtained for all six AFs with 10% methanol. The adsorption time was also evaluated. The
5 recoveries (Figure 3c) for all the analytes were satisfactory when the sample solution was mildly
6 shaken for 0.5–5 min. A longer period significantly reduced the recoveries of the target analytes.
7 This phenomenon is due to the fact that the organic solvents (methanol) and co-extracts may
8 break antibody or antigen–antibody interaction with a longer time. Therefore, an adsorption time
9 of 0.5 min was chose. The desorption conditions were also evaluated. The effect of the volume of
10 desorption solution (Figure 3d) on the desorption efficiency of the analytes was determined.
11 When 1 mL of methanol was used, the analytes were almost completely desorbed from the
12 immunomagnetic adsorbent. The time for desorption was also investigated, ranging from 5 to 60
13 s, with vortexing. The desorption time had no obvious effect on the extraction efficiency.
14 Therefore, a desorption time of 5 s was used. These results indicate that the desorption process is
15 quick and efficient, which may be attributable to the fact that methanol is highly destructive of
16 the antigen–antibody interaction. Finally, under the optimized conditions, the whole purification
17 procedure developed here only took less than 1 min, whereas it takes more than 1 h to pass the 60
18 mL of loading solution and 20 mL of washing solution through an IAC/SPE column at a flow rate
19 of 1 mL min⁻¹. Therefore, the new nanoarchiterture is a very time-efficient pretreatment process.
20 The reusability of the immunomagnetic adsorbent was also evaluated with regeneration and
21 cycling tests. After regeneration with PBS, the adsorption capacity of AFs-mAb/CTS/Fe₃O₄ was
22 almost constant in 10 continuous adsorption cycles. Therefore, it is clear that the
23 AFs-mAb/CTS/Fe₃O₄ immunosorbent can be reused, reflecting the excellent stability of the

1 antibodies on the surfaces of magnetic CTS beads. This outstanding reusability means that the
2 new nanomaterial can be regarded as a potential alternative to the enrichment of AFs.

3 **Method Validation.** A matrix effect (signal suppression/enhancement) is commonly
4 encountered in conventional approaches, eg. LC–MS analyses in the electrospray ionization
5 mode. When multiple compounds coelute with the target analyte, typical matrix suppression
6 effects and sometimes matrix enhancement effects can occur as a result of ionization
7 competition.¹⁴ In this case, the target content may be underestimated or overestimated when a
8 pure standard is used for quantification. Several measures have been proposed to minimize this
9 interference, including matrix-matched calibration,⁶ isotopic dilution,⁸ immunoaffinity
10 purification,¹⁵ and sample dilution.⁴¹ Immunoaffinity purification is the most popular technique
11 because its adsorption is specific. It has also been shown that matrix effects can be minimized or
12 eliminated using this selective extraction nanoarchitecture.⁴² In this study, the matrix effects based
13 on the slope ratios (R_{slope}) between the matrix-matched curves and the solvent standard curves
14 were investigated. The results indicate that little matrix suppression was observed for 6 AFs with
15 R_{slope} ranging from 0.832 to 1.109, which has been considered as matrix effects free and solvent
16 standard curves can be used for quantification.⁴¹ The mean recoveries for the six AF when
17 samples of corn, rice, wheat, peanut, peanut oil, sunflower oil, and olive oil were spiked with
18 three concentrations (1.0, 5.0 and 10.0 $\mu\text{g kg}^{-1}$) of AFs were in the range of 63%–118%. The
19 repeatability (intra-day precision) was less than 10.7%, and the within-laboratory reproducibility
20 (inter-day precision) did not exceed 16.3% (Table 1), which were expressed as relative standard
21 deviations (RSDs). Typical chromatograms for corn fortified with the six AF compounds (1.0 μg
22 kg^{-1}) are shown in Figure S5. The limits of detection (LODs) based on three times the
23 signal-to-noise ratio were in the range of 0.003–0.007 $\mu\text{g kg}^{-1}$ and the limits of quantification

1 (LOQs) based on 10 times the signal-to-noise ratio were in the range of 0.009–0.023 $\mu\text{g kg}^{-1}$.
2 Thus, the nanoarchitecture developed here is about 10-fold more sensitive than the IAC⁴³ and SPE
3 methods.⁴⁴

4 **Applications.** Finally to evaluate the reliability of the developed nanoarchitecture, three
5 certificated real foodstuffs were used to validate it: one brown rice and two corn powder samples.
6 The results are shown in Table 2. The brown rice sample was contaminated with 7.4 $\mu\text{g kg}^{-1}$
7 AFB₁, 0.2 $\mu\text{g kg}^{-1}$ AFB₂, and 0.5 $\mu\text{g kg}^{-1}$ AFM₁. AFB₁, AFB₂, AFG₁, and AFM₁ were detected in
8 the 1# corn sample at concentrations of 7.1, 0.7, 0.3, and 0.6 $\mu\text{g kg}^{-1}$, respectively. Five AFs were
9 found in the 2# corn sample, at concentrations of 17.7, 1.5, 0.4, 1.8, and 0.1 $\mu\text{g kg}^{-1}$ for AFB₁,
10 AFB₂, AFG₁, AFM₁, and AFM₂, respectively. No sample was contaminated with AFG₂. The
11 results for AFB₁, AFB₂, and AFG₂ using immunomagnetic separation agreed well with the
12 certified values³² and those obtained with the IAC method.³³ The AFB₂ detected in the brown rice
13 sample and the AFG₁ detected in the corn sample were below the LOD (0.5 $\mu\text{g kg}^{-1}$) of the
14 Association of Official Analytical Chemists (AOAC) Official Method 994.08. However, there was
15 no significant difference between the results for AFB₂ and AFG₁ when the IAC and
16 AFs-mAb/CTS/Fe₃O₄ methods were used. Three samples were also contaminated with AFM₁ and
17 AFM₂, with maximal contents of 1.8 and 0.2 $\mu\text{g kg}^{-1}$, respectively. Huang et al.⁶ and Han et al.⁸
18 also detected AFM₁ and AFM₂ in peanuts and traditional Chinese medical materials. It is
19 noteworthy that AFM₁ and AFM₂ are not only regarded as metabolites occurring in foods of
20 animal origin, but are also found in plant-derived foodstuffs. Taking into account all these factors,
21 the current UPLC–MS/MS method based on the AFs-mAb/CTS/Fe₃O₄ extraction procedure
22 developed in this study can be regarded as highly selective, sensitive, and effective for the
23 detection of six AFs in food samples.

1 ■ CONCLUSIONS

2 A multifunctional nanostructured architecture has been successfully fabricated by a facile
3 approach. The nanocomposite is composed of a magnetic Fe₃O₄ core, a middle layer of CTS and
4 the shell of AFs monoclonal antibody. Such design can fast and efficiently enrich extremely
5 low-level AFs contaminants in different foodstuffs, which can cause liver cancers. Magnetic
6 separation greatly improved the phase separation, while avoiding the time-consuming
7 requirement in the conventional approaches, eg. passaging through an IAC or SPE cartridge.
8 Because CTS/Fe₃O₄ nanoparticle have high adsorption capacities (23.5 mg g⁻¹) and high coupling
9 rates (more than 90%), a small amount of immunomagnetic absorbents (0.3 mL) can be used and
10 only half a minute is required to extract the analyte from the samples. Our results indicate that
11 this new strategy developed here is very efficient and sensitive, with potential application to
12 purification of trace contaminants in foodstuffs which are detrimental to human health.

13 ■ ASSOCIATED CONTENT

14 **Supporting Information**

15 Synthesis and characterization of CTS/Fe₃O₄ and Fe₃O₄ ; SPE and IAC separation used in
16 application procedure; UPLC–MS/MS detection; preparation of the broad-spectrum monoclonal
17 antibody (mAb) against AFs; and additional references. The Supporting Information is available
18 free of charge on the ACS Publications website.

19 ■ AUTHOR INFORMATION

20 **Corresponding Author**

21 * E-mail: shaobingch@sina.com. Phone: +86 10 62733875. Fax: +86 10 62731032.

22 * E-mail: junwang.tang@ucl.ac.uk. Phone: +44 (0)20 7679 7393. Fax: +44 (0)20 7383 2348.

23 **Author Contributions**

1 All authors have given approval to the final version of the manuscript.

2 ¹ These authors contributed equally to this work.

3 **Notes**

4 The authors declare no competing financial interest.

5 **■ ACKNOWLEDGMENTS**

6 This study was supported financially by grants from National Natural Science Foundation of
7 China (31672600), and the Science and Technology Planning Project of Zhangjiagang
8 (ZKS1506).

9 **■ REFERENCES**

- 10 (1) American Cancer Society, Global Cancer Facts & Figures, *American Cancer Society* **2007**, Atlanta, GA.
- 11 (2) Thun, M.J.; DeLancey, J.O.; Center, M.M.; Jemal, A.E.; Ward, M. *Carcinogenesis* **2010**, 31 (1), 100–110.
- 12 (3) Carlson, M.A.; Barger, C.B.; Benson, R.C.; Fraser, A.B.; Phillips, T.E.; Velky, J.T.; Groopman, J.D.; Strickland, P.T.; Ko,
13 H.W. *Biosens. Bioelectron.* **2000**, 14, 841–848.
- 14 (4) Amaike, S.; Keller, N.P. *Annu. Rev. Phytopath.* **2011**, 49, 107–133.
- 15 (5) Lewis, L.; Onsongo, M.; Njapau, H.; Schurz Rogers, H.; Lubber, G.; Kieszak, S.; Nyamongo, J.; Backer, L.; Dahiye, A.M.;
16 Misore, A.; DeCock, K.; Rubin, C.; and the Kenya Aflatoxicosis Investigation Group. *Environ. Health. Perspect.* **2005**, 113, 1763–
17 1767.
- 18 (6) Huang, B., Han, Z., Cai, Z., Wu, Y., Ren, Y., *Anal. Chim. Acta* **2010**, 662, 62–68.
- 19 (7) IARC Monograph on the Evaluation of Carcinogenic Risks to Humans, **2002** (82), IARC Press, Lyon.
- 20 (8) Han, Z.; Zheng, Y.; Luan, L.; Cai, Z.; Ren, Y.; Wu, Y. *Anal. Chim. Acta* **2010**, 664, 165–171.
- 21 (9) Ma, H.H.; Sun, J.Z.; Zhang, Y.; Bian, C.; Xia, S.H.; Zhen, T. *Biosens. Bioelectron.* **2016**, 80, 222–229.
- 22 (10) CAST, Mycotoxins: Risks in Plant, Animal, and Human Systems, *Council for Agricultural Science and Technology*, **2003**,
23 Ames, Iowa, USA.
- 24 (11) Chinese National Standard. **2011**, GB 2761-2011 maximum levels of mycotoxins in food.
- 25 (12) Codex Alimentarius Commission. **2001**, Codex Committee on food additives and contaminants 33rd session, Hague, The
26 Netherlands.
- 27 (13) European Commission, **2006**. Commission Regulation No. 1881/2006 of December 19th (2006). Setting maximum levels of
28 certain contaminants in foodstuffs. Official Journal of the European Union No. L364/5 of December 20th.

- 1 (14) Matuszewski, B.K.; Constanzer, M.L.; Chavez-Eng, C.M. *Anal. Chem.* **2003**, 75, 3019–3030.
- 2 (15) Turner, N.W.; Subrahmanyam, S.; Piletsky, S.A. *Anal. Chim. Acta* **2009**, 632, 168–180.
- 3 (16) Veach, B.T.; Mudalige, T.K.; Rye, P. *Anal. Chem.* **2017**, 89, 3256–3260.
- 4 (17) Gionfriddo, E.; Boyac, E.; Pawliszyn, J. *Anal. Chem.* **2017**, 89, 4046–4054.
- 5 (18) Xiong, K.; Wei, W.; Jin, Y.J.; Wang, S.M.; Zhao, D.X.; Wang, S.; Gao, X.Y.; Qiao, C.M.; Yue, H.; Ma, G.H.; Xie, H.Y. *Adv.*
6 *Mater.* **2016**, 28, 7929–7935.
- 7 (19) Yang, H.W.; Lin, C.W.; Hua, M.Y.; Liao, S.S.; Chen, Y.T.; Chen, H.C.; Weng, W.H.; Chuang, C.K.; Pang, S.T.; Ma, C.C.M.
8 *Adv. Mater.* **2014**, 26, 3662–3666.
- 9 (20) Pappert, G.; Rieger, M.; Niessner, R.; Seidel, M. *Microchim. Acta* **2010**, 168, 1–8.
- 10 (21) Baniukevic, J.; Hakki Boyaci, I.; Goktug Bozkurt, A.; Tamer, U.; Ramanavicius, A.; Ramanaviciene, A. *Biosens.*
11 *Bioelectron.* **2013**, 43, 281–288.
- 12 (22) Speroni, F.; Elviri, L.; Careri, M.; Mangia, A. *Anal. Bioanal. Chem.* **2010**, 397, 3035–3042.
- 13 (23) de Souza Castilho, M.; Laube, T.; Yamanaka, H.; Alegret, S.; Pividori, M.I. *Anal. Chem.* **2011**, 83 (14), 5570–5577.
- 14 (24) Xiao, Q.; Li, H.; Hu, G.; Wang, H.; Li, Z.; Lin, J.M. *Clin. Biochem.* **2009**, 42 (13-14), 1461–1467.
- 15 (25) Xie, F.; Lai, W.; Saini, J.; Shan, S.; Cui, X.; Liu, D. *Food Chem.* **2014**, 150, 99–105.
- 16 (26) Xiong, Y.; Tu, Z.; Huang, X.; Xie, B.; Xiong, Y.; Xu, Y. *RSC Adv.* **2015**, 5, 77380–77387.
- 17 (27) Jiang, W.; Wang, W.; Pan, B.; Zhang, Q.; Zhang, W.; Lv, L. *ACS Appl. Mater. Inter.* **2014**, 6, 3421–3426.
- 18 (28) Arias, J.L.; Reddy, L.H.; Couvreur, P. *J. Mater. Chem.* **2012**, 22, 7622–7632.
- 19 (29) Liu, Q.; Yang, C.; Chen, J.; Jiang, B. *J. Control. Release* **2011**, 152, e250–e269.
- 20 (30) Wang, Y.; Wang, X.; Luo, G.; Dai, Y. *Bioresource Technol.* **2008**, 99, 3881–3884.
- 21 (31) Liu, T.; Xie, J.; Zhao, J.; Song, G.; Hu, Y. *Food Anal. Method* **2014**, 7, 814–819.
- 22 (32) AOAC Official Method 994.08.
- 23 (33) Xie, J.; Sun, Y.; Zheng, Y.; Wang, C.; Sun, S.; Li, J.; Ding, S.; Xia, X.; Jiang, H. *Food Control* **2017**, 73, 445–451.
- 24 (34) Urusov, A.E.; Petrakova, A.V.; Vozniak, M.V.; Zherdev, A.V.; Dzantiev, B.B. *Sensors* **2014**, 14, 21843–21857.
- 25 (35) Zhang S.; Wang J.; Li D.; Huang J.; Yang H.; Deng A. *Talanta* **2010**, 82, 704–709.
- 26 (36) Yao, K.; Zhang, W.; Yang, L.; Gong, J.; Li, L.; Jin, T.; Li, C. *J. Chromatogr. B* **2015**, 1003, 67–73.
- 27 (37) Mansur, H.S.; Mansur, A.A.P.; Soriano-Araújo, A.; Lobato, Z.I.P.; *Green Chem.* **2015**, 17, 1820–1830.
- 28 (38) Peng, Z.G.; Hidajat, K.; Uddin, M.S. *J. Colloid. Interf. Sci.* **2004**, 271, 277–283.
- 29 (39) Lee, W.; Ko, J.; Kim, H. *J. Colloid. Interf. Sci.* **2002**, 246, 70–77.
- 30 (40) Chun, K.; Stroeve, P. *Langmuir.* **2002**, 18, 4653–4658.
- 31 (41) Yang, P.; Chang, J.S.; Wong, J.W.; Zhang, K.; Krynetsky, A.J.; Bromirski, M.; Wang, J. *J. Agr. Food Chem.* **2015**, 63 (21),

- 1 5169–5177.
- 2 (42) Chen, D.Y.; Zhu, H.G.; Yang, S.; Li, N.J.; Xu, Q.F.; Li, H.; He, J.H.; Lu, J.M. *Adv. Mater.* **2016**, *28*, 10443–10458.
- 3 (43) Iha, M.H.; Mini, C.A.; Okada, I.A.; Briganti, R.C.; Trucksess, M.W. *J. Chromatogr. A* **2017**, *1483*, 1–7.
- 4 (44) Ran, C.C.; Chen, D.; Ma, H.Y.; Jiang, Y. *J. Chromatogr. B* **2017**, *1044-1045*, 120–126.

5

1 **Figure captions**

2 **Scheme 1.** A schematic illustration of the procedure used to synthesize the AFs-mAb/CTS/Fe₃O₄
3 nanoarchitecture and its application.

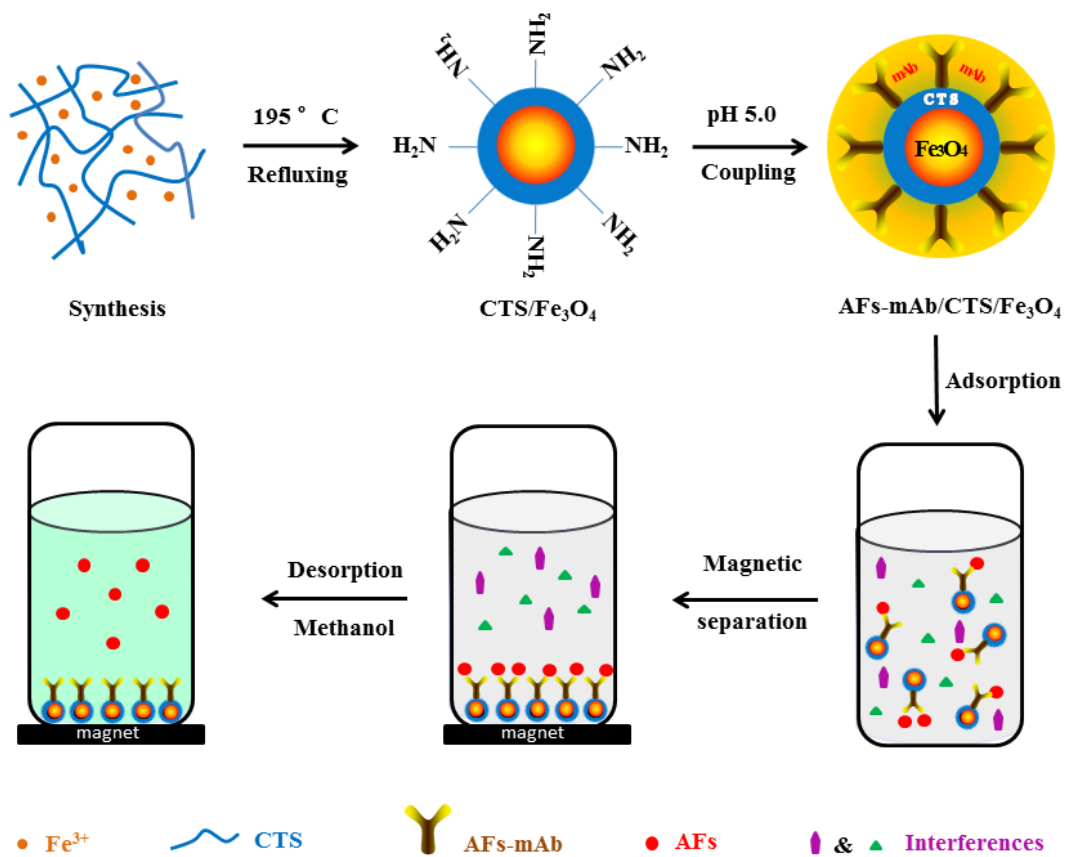
4 **Figure 1.** (a) XRD curves for CTS/Fe₃O₄, Fe₃O₄, and CTS; (b) SEM image of CTS/Fe₃O₄; (c) TEM images of
5 CTS/Fe₃O₄ and Fe₃O₄; (d) FTIR curves for CTS/Fe₃O₄, Fe₃O₄, and CTS.

6 **Figure 2.** Optimized preparation of the immunomagnetic absorbent (n = 3). (a) The coupling efficiency
7 achieved with different coupling methods: GA, glutaraldehyde method; ESA, electrostatic adsorption method;
8 EDC/sulfo-NHS, 1-ethyl-3-(3-dimethylaminopropyl)-carbodiimide/N-hydroxysulfosuccinimide method. (b)
9 The coupling efficiency with different concentrations of coupling solution. (c) The coupling efficiency
10 achieved with coupling solution of different pHs. (d) Effect of reaction time on the coupling process.

11 **Figure 3.** Optimized extraction procedure of the immunomagnetic absorbent (n = 3) in corn samples spiked
12 with AFs concentration of 1.0 µg kg⁻¹. (a) Recovery curve for AFs with different amounts of immunomagnetic
13 beads. (b) Recovery curve for AFs with different ratios of methanol in the loading solution. (c) Effect of
14 loading time on the recognition of AFs by immunomagnetic beads. (d) Recovery variation curve with different
15 volumes of elution solution. Evaluations were performed as for other types of samples.

16

1 Scheme 1

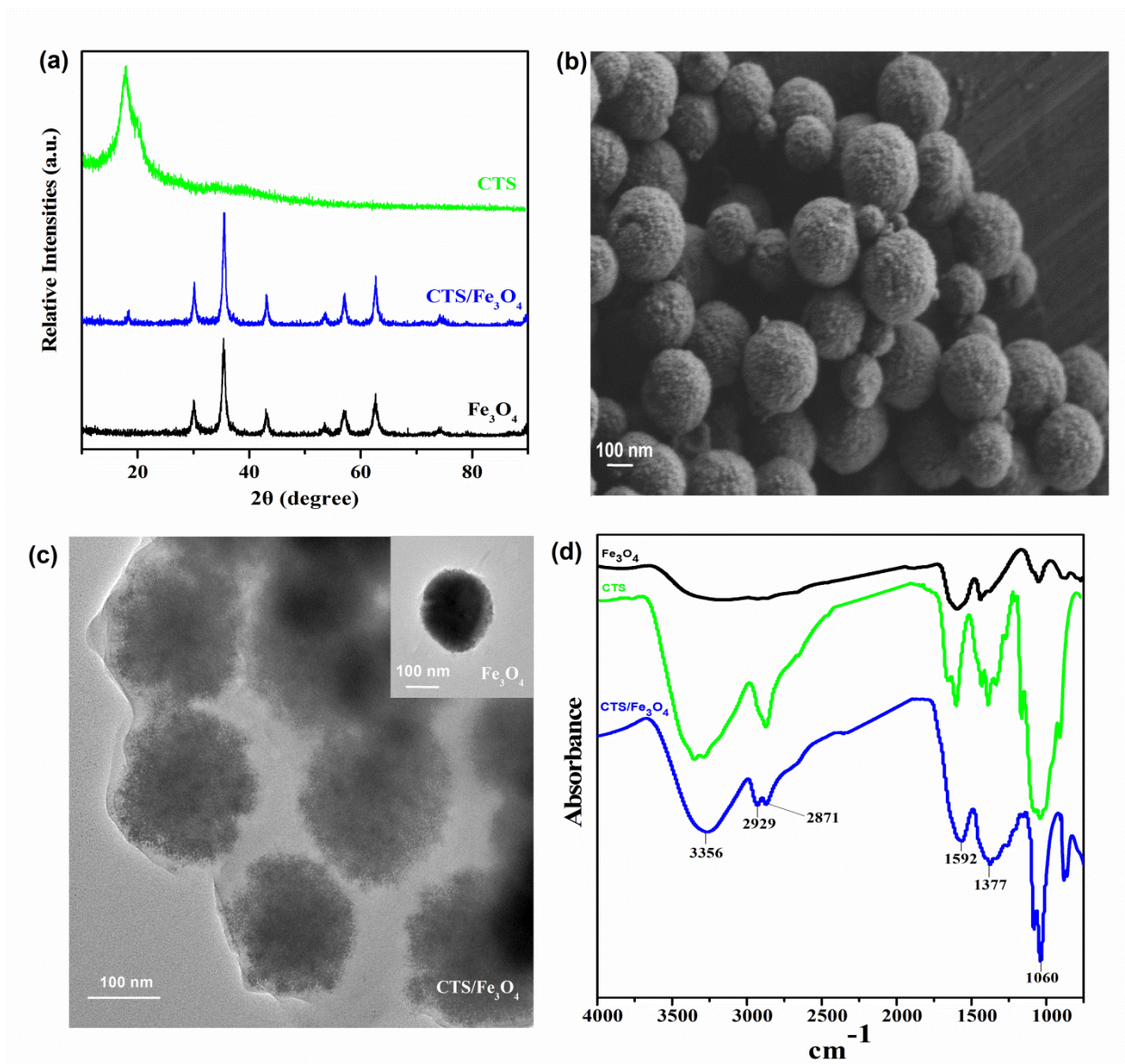


2

3

4

1 **Figure 1**

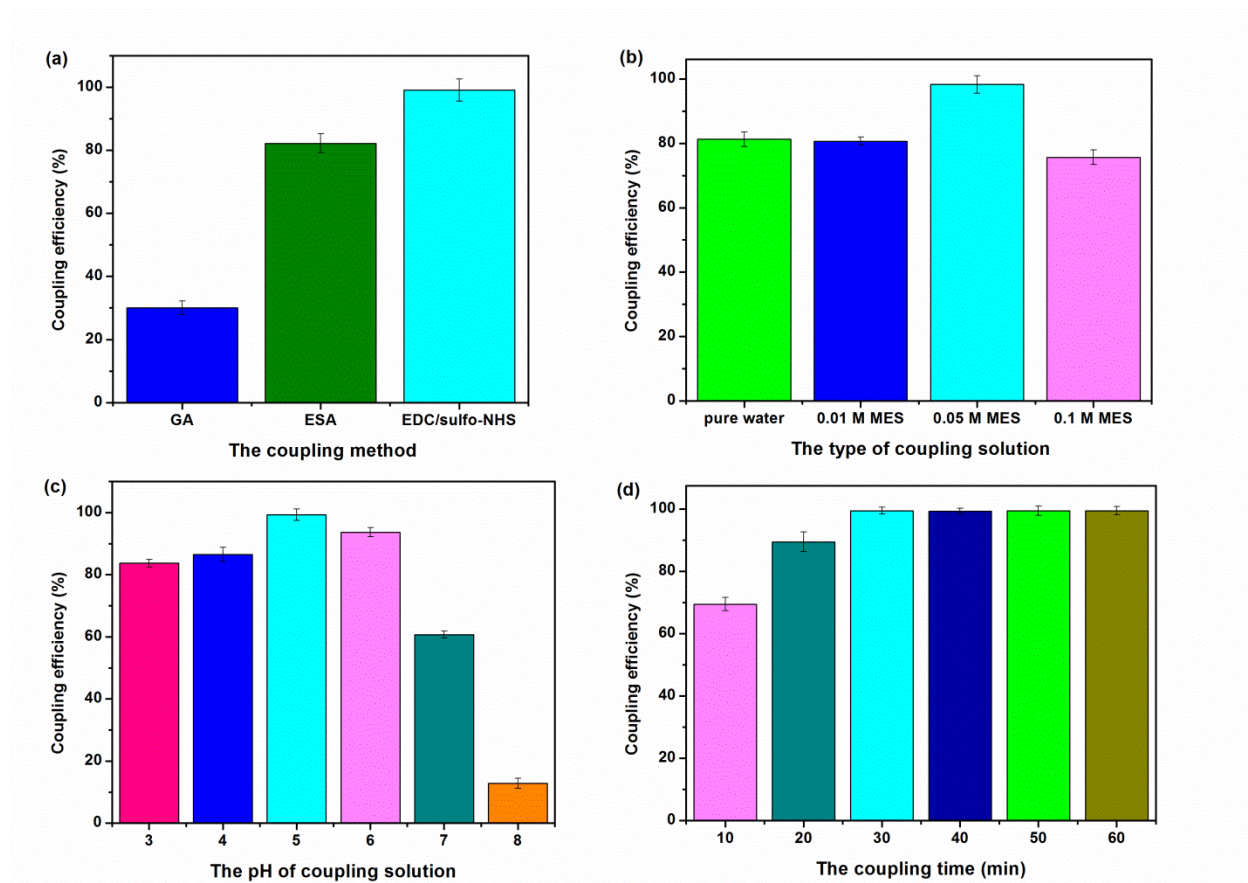


2

3

4

1 **Figure 2**

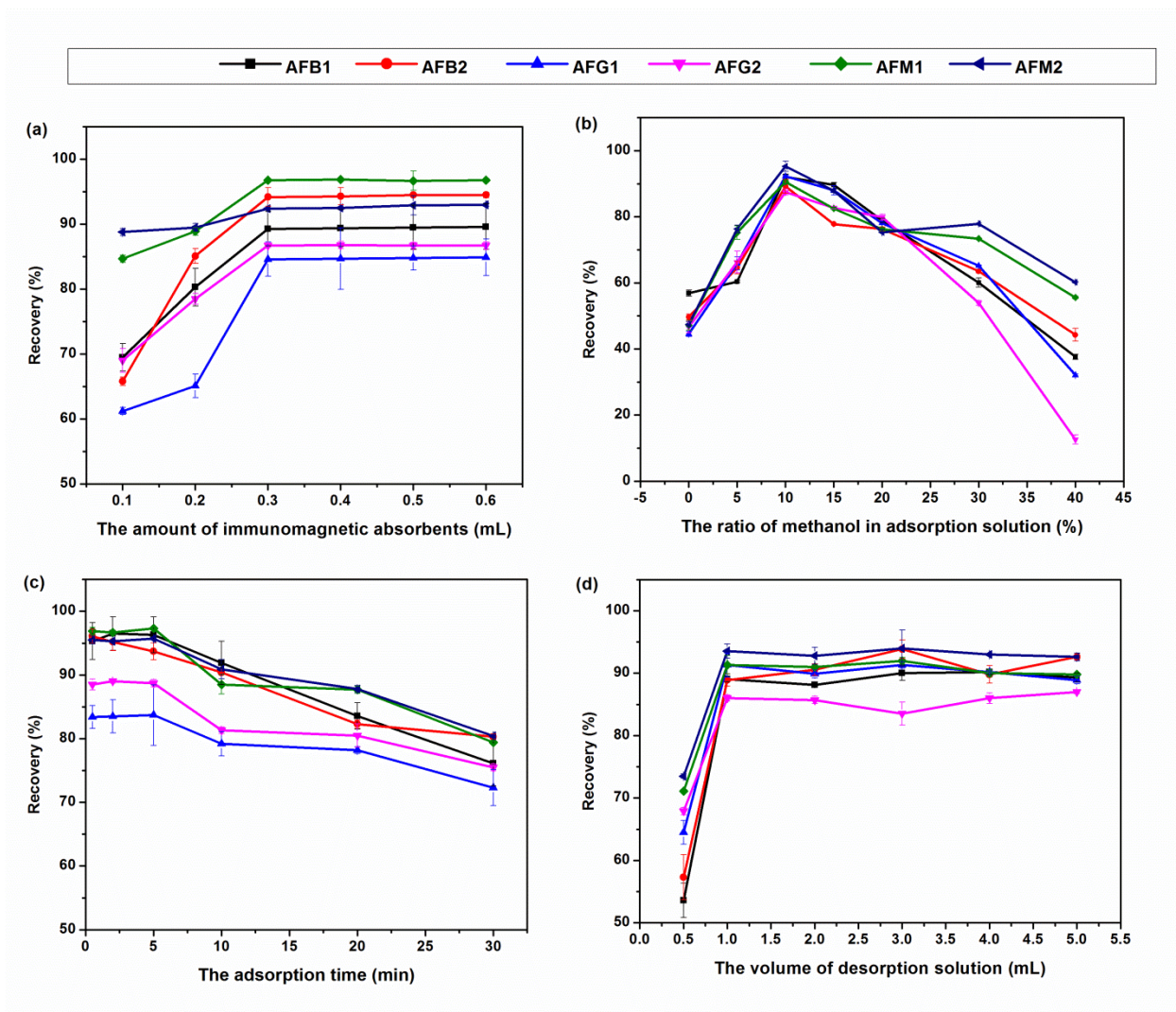


2

3

4

1 **Figure 3**



2

3

4

Table 1. LODs, LOQs, mean recoveries, repeatability and reproducibility of AFs (n = 3).

Compounds	LOD ($\mu\text{g kg}^{-1}$)	LOQ ($\mu\text{g kg}^{-1}$)	Added ($\mu\text{g kg}^{-1}$)	Mean recoveries (intra-/inter-, RSDs) (%)						
				Corn	Rice	Wheat	Peanut	Peanut oil	Sunflower oil	Olive oil
AFB ₁	0.003	0.009	1.0	86 (7.6/9.1)	99 (3.7/8.9)	82 (7.1/9.5)	78 (4.3/11.2)	98 (8.0/13.2)	101 (5.1/6.5)	83 (7.6/9.7)
			5.0	92 (9.3/12.0)	83 (3.5/6.7)	88 (8.7/10.7)	92 (6.8/7.5)	105 (5.1/8.8)	89 (4.7/8.2)	98 (7.3/12.3)
			10.0	87 (5.3/7.4)	107 (4.2/6.3)	91 (6.8/9.5)	82 (5.9/7.3)	92 (6.4/10.3)	104 (6.9/13.0)	108 (9.3/11.5)
AFB ₂	0.003	0.012	1.0	78 (2.1/5.2)	86 (4.6/7.3)	78 (10.2/12.6)	106 (3.8/6.2)	118 (3.3/5.2)	84 (9.3/9.8)	83 (3.2/5.1)
			5.0	69 (7.2/7.7)	98 (7.3/10.4)	92 (7.6/13.8)	86 (8.4/11.2)	100 (5.6/7.1)	83 (9.1/12.7)	86 (4.6/9.5)
			10.0	91 (9.3/10.4)	98 (8.2/15.8)	81 (3.3/7.4)	99 (4.5/8.3)	91 (3.4/7.2)	97 (7.2/11.9)	97 (9.4/13.6)
AFG ₁	0.005	0.017	1.0	85 (6.6/8.9)	85 (9.5/12.5)	98 (5.4/6.9)	112 (5.7/8.6)	92 (8.3/9.0)	84 (7.5/8.3)	89 (8.3/14.2)
			5.0	97 (6.7/9.2)	97 (8.9/10.6)	87 (6.6/7.5)	76 (6.4/7.7)	98 (4.6/5.1)	87 (5.9/11.9)	106 (7.6/9.0)
			10.0	73 (8.2/12.8)	107 (6.5/6.8)	83 (9.6/13.7)	87 (7.5/9.4)	79 (3.7/8.8)	89 (6.5/7.3)	109 (10.7/11.5)
AFG ₂	0.007	0.023	1.0	86 (7.5/9.6)	94 (2.6/7.8)	98 (3.9/8.4)	87 (6.7/11.5)	78 (5.6/9.2)	75 (9.1/10.4)	104 (6.2/8.5)
			5.0	87 (4.6/7.7)	99 (6.5/8.4)	93 (7.2/12.6)	85 (7.8/9.9)	97 (10.2/16.3)	69 (6.5/8.3)	87 (6.7/9.1)
			10.0	96 (4.2/6.4)	97 (7.8/9.2)	91 (10.1/14.7)	83 (6.1/8.5)	88 (5.9/7.4)	77 (4.2/8.9)	95 (7.4/9.3)
AFM ₁	0.006	0.021	1.0	88 (6.2/7.8)	98 (4.2/5.4)	79 (3.4/7.5)	103 (4.9/8.3)	65 (2.2/6.6)	102 (9.2/15.8)	63 (6.4/7.3)
			5.0	103 (9.2/11.5)	99 (8.5/13.9)	88 (8.3/9.8)	95 (7.1/8.5)	77 (3.6/7.2)	85 (3.9/9.6)	82 (9.5/12.7)
			10.0	96 (5.5/8.6)	91 (9.2/10.5)	82 (7.6/11.6)	97 (9.8/11.2)	83 (9.8/13.8)	74 (5.3/7.3)	99 (7.6/8.1)
AFM ₂	0.005	0.018	1.0	82 (4.5/6.5)	89 (7.3/9.2)	67 (4.1/4.8)	93 (6.7/8.5)	72 (8.3/12.9)	84 (6.2/7.8)	80 (5.6/12.9)
			5.0	81 (7.5/8.1)	84 (8.9/9.5)	71 (9.3/10.8)	104 (9.6/13.7)	87 (5.2/7.3)	83 (9.9/15.0)	95 (8.2/10.4)
			10.0	108 (5.9/8.5)	102 (7.9/11.6)	82 (7.4/9.8)	98 (8.5/15.6)	89 (6.5/9.3)	86 (3.8/8.2)	91 (8.6/14.6)

Table 2. Validated results for real-life specimens using SPE, IAC, and AFs-mAb/CTS/Fe₃O₄.

Samples	Methods	Concentrations ($\mu\text{g kg}^{-1}$)					
		AFB ₁	AFB ₂	AFG ₁	AFG ₂	AFM ₁	AFM ₂
Brown rice	SPE ^{a)}		6.4~8.6 ^{b)}			- ^{c)}	-
		7.5	ND	ND	ND	-	-
	IAC ^{e)}		8.0 ^{f)}				
		7.7	0.3	ND	ND	0.4	ND
AFs-mAb/CTS/Fe ₃ O ₄		7.6 ^{g)}					
	7.4	0.2	ND	ND	0.5	ND	
1# Corn	SPE		6.8~12.0 ^{b)}			-	-
		8.6	0.8	ND	ND	-	-
	IAC		7.7 ^{f)}				
		6.9	0.6	0.2	ND	0.7	ND
AFs-mAb/CTS/Fe ₃ O ₄		8.1 ^{g)}					
	7.1	0.7	0.3	ND	0.6	ND	
2# Corn	SPE		14.8~27.2 ^{b)}			-	-
		19.1	1.9	ND	ND	-	-
	IAC		20.2 ^{f)}				
		18.2	1.4	0.6	ND	1.5	0.2
AFs-mAb/CTS/Fe ₃ O ₄		19.6 ^{g)}					
	17.7	1.5	0.4	ND	1.8	0.1	

^{a)} The results were obtained from Trilogy Analytical Laboratory Inc. (Washington, MO, USA) with HPLC using AOAC Official Method 994.08, with modifications.³² The detection limits were 0.5 $\mu\text{g kg}^{-1}$ for AFB₁, AFB₂, AFG₁, AFG₂; ^{b)} Range of product incorporating uncertainty ranges for the total of AFB₁, AFB₂, AFG₁ and AFG₂; ^{c)} Data not given; ^{d)} ND= not detected; ^{e)} IAC method using the same pretreatment procedure as in our previous study, with some modifications;³³ ^{f)} The total values for AFB₁, AFB₂, AFG₁, and AFG₂ determined with the IAC method; ^{g)} The total values for AFB₁, AFB₂, AFG₁, and AFG₂ determined with the nanoarchitecture developed in this study.

For TOC only

